Analytical and experimental study on aerodynamic control of flutter and buffeting of bridge deck by using mechanically driven flaps

Duc - Huynh Phan[*1] and Hiroshi Kobayshi[2a]

[1]*Department of Civil Engineering, the University of Education and Technology, VietNam*
[2]*Ritsumeikan University, Japan*

Abstract.   A passive control using flaps will be an alternative solution for flutter stability and buffeting response of a long suspension bridge. This method not only enables a lightweight economic stiffening girder without an additional stiffness for aerodynamic stability but also avoid the problems from the malfunctions of control systems and energy supply system of an active control by winglets and flaps. A time domain approach for predicting the coupled flutter and buffeting response of bridge deck with flaps is investigated. First, the flutter derivatives of bridge deck and flaps are found by experiment. Next, the derivation of time domain model of self-excited forces and control forces of sectional model is reported by using the rational function approximation. Finally, the effectiveness of passive flap control is investigated by the numerical simulation. The results show that the passive control by using flaps can increase the flutter speed and decrease the buffeting response. The experiment results are matched with numerical ones.

Keywords: flutter, buffeting, suspension bridge, passive control, flaps, rational function approximation

1. Introduction

Rapid technological progress in bridge engineering has led to the construction of the Akashi Kaikyo Bridge in Japan (main span of 1990m), the Great Belt Bridge in Denmark (main span of 1624m), and the Messina Strait bridge (under construction with main span of 3300m). It is believed that in the future designs with improved girder forms, lightweight cables, and control devices may be up to 5000 m long. For such extremely long bridges, besides problems of strength of material (cable); economic design (lightweight deck); seismic safety (earthquake); structure-wind interaction phenomena, static as well as dynamic, which are increasingly important as spans become longer and bridge girders more flexible, may be a serious problem – flutter and buffeting, especially when the girder depth-to-width ratio is small compared with existing long bridges.

One of the promising solutions for flutter and buffeting control is the change of the cross section, for instance, a multi-box cross section. The aerodynamic advantages of this solution have

---

∗Corresponding author, Ph.D., E-mail: huynhpd@hcmute.edu.vn
[a]Professor emeritus

been exploited in the multi-box cross section design of the proposed 3,300 m span suspension bridge for the crossing of the Messina Strait (Brown 1996, 1999, Matsumoto *et al.* 2007). Another proposal for Japanese project is 2-box with slot girder (Sato *et al.* 2000, 2002).

For suspension bridges with a main span of several kilometers, active methods to achieve the aerodynamic stability can provide a new design alternative. The application of the active mass driver was studied (Dung *et al.* 1996, Miyata *et al.* 1994). Körlin and Starossek (2007) also proposed the active mass damper to enhance the flutter stability. With linear control, the measured critical wind speed of the sectional model rises by about 16.5% (Körlin and Starossek 2007).

The passive aerodynamic control is more attractive from a practical point of view. If a proper mechanism for a passive system is invented, it can easily be applied to the actual bridge because of its simplicity and reliability. One kind of the passive system is the tuned mass damper TMD was examined (Okada *et al.* 1998, Lin *et al.* 2000, Kwon *et al.* 2000, 2004, Gua *et al.* 1998, 2001, 2002), and its performance was proven to be effective against flutter and buffeting. Vaurigaud *et al.* (2011) also proposed a passive control by using nonlinear energy sink. The analytical calculations showed that this control method was able to efficiently control the aeroelastic instability of the bridge.

In the above references, the flutter suppression methods are based on the structural mechanics. Modifying the flow around the bridge deck or generating stabilizing aerodynamic forces from the flow is another approach to the flutter problem.

The researches on aerodynamic control by using winglets and flaps or being called control surfaces were proposed and developed (Kobayashi and Nagaoka 1992, Kobayashi and Nitta 1996, Kobayashi *et al.* 1998, Kobayashi *et al.* 2001, Kobayashi and Phan 2005, Phan and Kobayashi 2011). An extensive theoretical study on the active control of bridge flutter using a model similar to that proposed by Kobayashi was presented (Wilde and Fujino 1998, Preidikman and Mook 1998, Nissen *et al.* 2004, Kirch *et al.* 2009). They also translated their active model to a passive one (Wilde *et al.* 1999). This model consists of two control surfaces attached to both edges of the deck and a pendulum placed inside the deck. The maximum improvement of the flutter speed is 43%. The buffeting effect was not considered yet. Omenzetter *et al.* (2000, 2002) also proposed the passive flap control with springs and supplementary cables. They showed the numerical result, but the experimental study was not yet shown.

This study investigates the efficiency of passive flaps (mechanically driven flap) for controlling of flutter and buffeting of a bridge deck. A flap is mechanically controlled after a pitching motion of the deck and the aerodynamic damping or suppressing aerodynamic force is produced. A time domain approach for predicting the coupled flutter and buffeting response of bridge deck with flaps is investigated. First, the flutter derivatives of bridge deck and flaps are found by experiment. Next, the derivation of time domain model of self-excited forces and control forces of sectional model is reported by using the rational function approximation technique known as Roger's approximation. Finally, the effectiveness of passive flap control is investigated by the numerical simulation. The results show that the passive control by using flaps can increase the flutter speed and decrease the buffeting response. The experiment results are matched with numerical ones.

2. Bridge deck with mechanically driven flap

Turning the flap mechanically in proportion to the bridge deck torsion displacement is easily realized in a suspension bridge. Fig. 1 shows the bridge deck system having flaps which are

mechanically driven after the rotational motion of the deck. Fig. 2 shows the sketch of the flap driving mechanism. In these figures, h is the vertical displacement of bridge deck, α is the angle of attack of the bridge deck, β is the angle of the trailing edge flap, and γ is the angle of the leading edge flap. The flap is fixed with a hinge at the longitudinal edge of the bridge deck. Two hanger cables from a main cable are fixed to an anchor beam at its ends. A cross beam of the deck system is fixed to the anchor beam with a hinge.

The gears G_s and G_f are fastened to the anchor beam and flap, respectively. Both gears are connected by a driving belt. When a bridge deck causes a torsion motion in its natural oscillation mode, hanger ropes almost keep their vertical figure. The relative rotation angle is transmitted to the rotation of the flap through the driving belt with a given amplifying factor $G = R_s/R_f$ where R_s and R_f are the radiuses of the gear G_s and G_f, respectively. Thus the flap is driven just after the pitching motion of the bridge deck mechanically.

The same mechanism of flap driving system is installed at the leeward side of the bridge deck. When the flaps are driven through the above mentioned manner, if we set the head-up motion of the bridge deck as α, the turning down of leading edge flap is $\gamma = G\alpha$ and the turning up the trailing edge flap is $\beta = -G\alpha$. The same flap motions are seen when the wind direction is reversed.

Such driving system is installed at the position of every hanger cable where a flap is thought to be required for the control of bridge deck oscillation. The length of a fraction of the flap corresponds to the distance between the hanger ropes. The flaps are installed avoiding the center of the main span of suspension bridge. Because the short hanger ropes near the center of a main span of a suspension bridge rotate with the rotational motion of the bridge deck, the relative rotation angle between the anchor beam and the cross beam is difficult to be appeared.
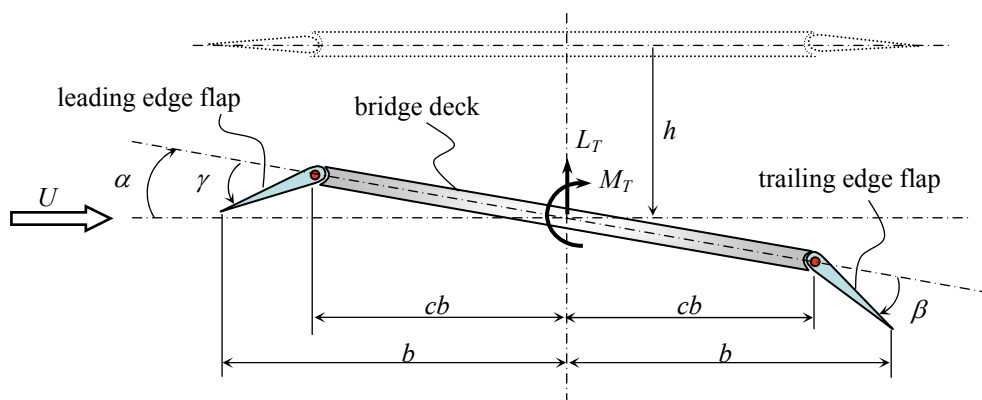
If the different amplification factors among the leeward and the windward flaps are required, $\gamma = X\alpha$, $\beta = Y\alpha$. where X and Y are amplification factors, the wind-detecting apparatus is used and driving mechanism is switched to the other one following the wind direction. The friction damping by the mechanism is also expected as a stabilizing effect for the aerodynamic responses.

3. Experimental identification of self-excited forces and flapping forces

For the bluff bridge deck sections, the flutter derivatives must be determined experimentally.

Fig. 1 Bridge deck with flaps at leading and trailing edge

(a) Bridge with flaps

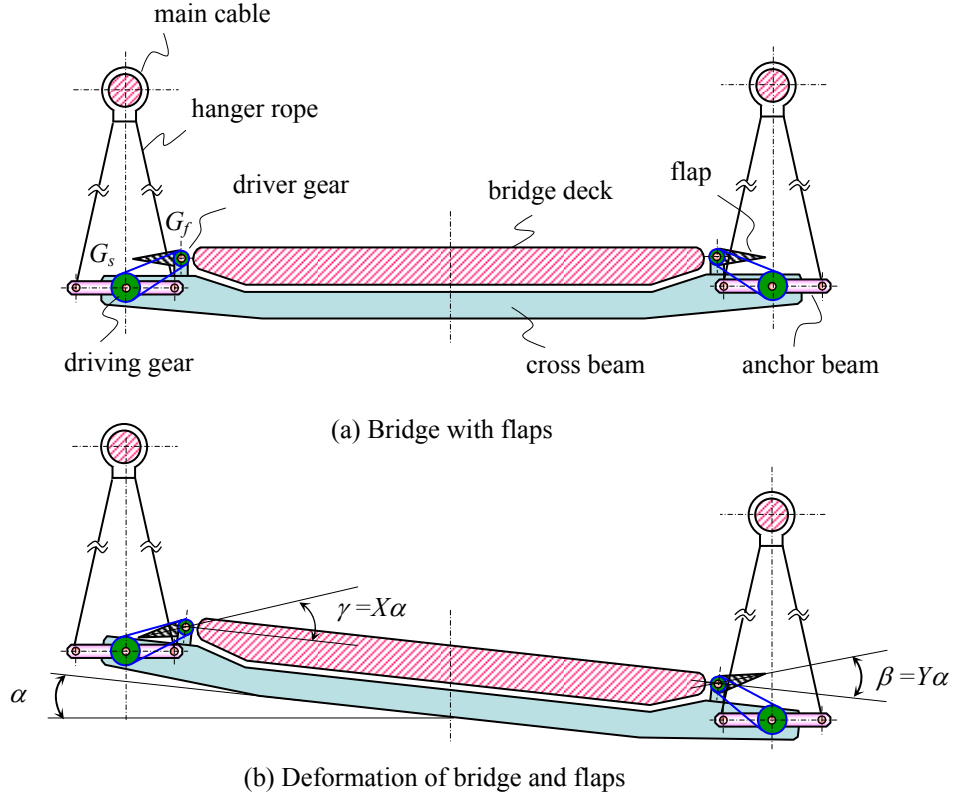(b) Deformation of bridge and flaps

Fig. 2 Bridge deck with mechanically driven flap

This is done through a system identification method in the frequency or time domain using free vibration or forced vibration testing in a wind tunnel. The drag component and the components associated with the lateral motion are negligible. In this section, the flutter derivatives of the self-excited forces of bridge deck and the ones of the control forces produced by flap motion are obtained experimentally.

3.1 Testing method

The governing equations of motion in the smooth flow with respect to the static equilibrium position of a two-dimensional bridge deck excited by aerodynamic forces are given by

$$\ddot{h} + 2\xi_h \omega_h \dot{h} + \omega_h^2 h = -\frac{L_T}{m} \qquad \ddot{\alpha} + 2\xi_\alpha \omega_\alpha \dot{\alpha} + \omega_\alpha^2 \alpha = \frac{M_T}{I} \tag{1}$$

In which m = mass per unit length; I = moment of inertial per unit length; ξ_h, ξ_α = damping ratios of heaving motion h and pitching motion α, respectively; ω_h, ω_α = natural circular frequencies of heaving and pitching motion, respectively; L_T = total aerodynamic lift force (positive when upward); M_T = total aerodynamic moment (positive when clockwise).

The total lift L_T and moment M_T are separated into their self-excited and control components

$$L_T = L_{se} + L_{ad} \quad M_T = M_{se} + M_{ad} \tag{2}$$

where L_{se} = self-excited lift; M_{se} = self-excited moment; L_{ad} = control lift; M_{ad} = control moment.

The self-excited forces per unit span can be expressed in the format below

$$L_{se} = \frac{1}{2}\rho U^2 B \left[H_1 \frac{\dot{h}}{U} + H_2 \frac{B\dot{\alpha}}{U} + H_3 \alpha + H_4 \frac{h}{B} \right]$$

$$M_{se} = \frac{1}{2}\rho U^2 B^2 \left[A_1 \frac{\dot{h}}{U} + A_2 \frac{B\dot{\alpha}}{U} + A_3 \alpha + A_4 \frac{h}{B} \right] \tag{3}$$

In which ρ = air density, U = wind speed, $B = 2b$ = bridge deck width. H_i and A_i (i = 1 to 4) are the unknown coefficients, they play the roles analogous to the steady-state coefficients like $dC_L/d\alpha$. The section model is spring-mounted in a smooth flow, given an initial displacement, and allowed an oscillation. Then, the system identification techniques are employed to identify the H_i and A_i.

If flaps are driven after pitching motion of bridge deck, the control forces can be expressed in the function of the velocity and the displacement of them

$$L_{ad} = \frac{1}{2}\rho U^2 B \left[F_{L1} \frac{B\dot{\gamma}}{U} + F_{L2} \frac{B\dot{\beta}}{U} + F_{L3}\gamma + F_{L4}\beta \right]$$

$$M_{ad} = \frac{1}{2}\rho U^2 B^2 \left[F_{M1} \frac{B\dot{\gamma}}{U} + F_{M2} \frac{B\dot{\beta}}{U} + F_{M3}\gamma + F_{M4}\beta \right] \tag{4}$$

where F_{Li} and F_{Mi} (i = 1 to 4) are the unknown coefficients.

With the above control manners, the leading edge flap and trailing edge flap relate to the pitching motion by

$$\gamma = X\alpha \quad \beta = Y\alpha \tag{5}$$

where X and Y are amplification factors of the leeward and the windward flaps, respectively.

Take the derivatives of Eq. (5), substituting them into Eq. (4), and take the sum of Eq. (3) and Eq. (4), the total lift and moment of Eq. (2) generally are

$$L_T = \frac{1}{2}\rho U^2 B \left[H_{10} \frac{\dot{h}}{U} + H_{20} \frac{B\dot{\alpha}}{U} + H_{30} \alpha + H_{40} \frac{h}{B} \right]$$

$$M_T = \frac{1}{2}\rho U^2 B^2 \left[A_{10} \frac{\dot{h}}{U} + A_{20} \frac{B\dot{\alpha}}{U} + A_{30} \alpha + A_{40} \frac{h}{B} \right] \tag{6}$$

where

$$H_{10} = H_1 \quad H_{20} = H_2 + F_{L1}X + F_{L2}Y \quad H_{30} = H_3 + F_{L3}X + F_{L4}Y \quad H_{40} = H_4$$

$$A_{10} = A_1 \quad A_{20} = A_2 + F_{M1}X + F_{M2}Y \quad A_{30} = A_3 + F_{M3}X + F_{M4}Y \quad A_{40} = A_4 \tag{7}$$

Generally, at a given wind velocity, the heaving, pitching, damping ratio, and frequency of bridge deck can be measured experimentally in the smooth flow. Then, the coefficients H_{i0} and A_{i0} can be found by using the least square method.

First, the experiment is performed with the fixed flaps, $X = Y = 0$. The coefficients H_i and A_i ($i = 1$ to 4) are obtained. Next, the trailing edge flap is fixed with $\beta = 0$ while the leading edge flap is driven with $\gamma = X\alpha$ ($X \neq 0$) at the given wind velocity, the following coefficients F_{L1}; F_{L3}; F_{M1}; F_{M3} are calculated from Eqs. (7)

$$F_{L1} = \frac{H_{20} - H_2}{X} \quad F_{L3} = \frac{H_{30} - H_3}{X} \quad F_{M1} = \frac{A_{20} - A_2}{X} \quad F_{M3} = \frac{A_{30} - A_3}{X} \tag{8}$$

Finally, the leading edge flap is fixed with $\gamma = 0$ while the trailing edge flap is driven with $\beta = Y\alpha$ ($Y \neq 0$) at given speed. From Eq. (7)

$$F_{L2} = \frac{H_{20} - H_2}{Y} \quad F_{L4} = \frac{H_{30} - H_3}{Y} \quad F_{M2} = \frac{A_{20} - A_2}{Y} \quad F_{M4} = \frac{A_{30} - A_3}{Y} \tag{9}$$

Generally, H_i and K_i are the functions of the reduced frequency $K = \omega B/U$. Eq. (3) and Eq. (4) are commonly described utilizing flutter derivatives as follows (Scanlan 1978)

$$L_{se} = \frac{1}{2}\rho U^2 B \left[K H_1^* \frac{\dot{h}}{U} + K H_2^* \frac{B\dot{\alpha}}{U} + K^2 H_3^* \alpha + K^2 H_4^* \frac{h}{B} \right]$$

$$M_{se} = \frac{1}{2}\rho U^2 B^2 \left[K A_1^* \frac{\dot{h}}{U} + K A_2^* \frac{B\dot{\alpha}}{U} + K^2 A_3^* \alpha + K^2 A_4^* \frac{h}{B} \right] \tag{10}$$

and

$$L_{ad} = \frac{1}{2}\rho U^2 B \left[K F_{L1}^* \frac{B\dot{\gamma}}{U} + K F_{L2}^* \frac{B\dot{\beta}}{U} + K^2 F_{L3}^* \gamma + K^2 F_{L4}^* \beta \right]$$

$$M_{ad} = \frac{1}{2}\rho U^2 B^2 \left[K F_{M1}^* \frac{B\dot{\gamma}}{U} + K F_{M2}^* \frac{B\dot{\beta}}{U} + K^2 F_{M3}^* \gamma + K^2 F_{M4}^* \beta \right] \tag{11}$$

where $H_i^*, A_i^*, F_{Li}^*, F_{Mi}^*$ ($i = 1$ to 4) = frequency dependent flutter derivatives. They can be calculated from H_i, A_i, F_{Li}, F_{Mi} ($i = 1$ to 4) of Eqs. (3) and Eq. (4).

3.2 Experimental model

To find the coefficients $H_i^*, A_i^*, F_{Li}^*, F_{Mi}^*$ ($i = 1$ to 4) of Eq. (10) and Eq. (11), the two dimensional wind tunnel test was done using a two dimensional bridge deck model with flaps. The cross sectional shape of the model and flaps are shown in Fig. 3(a). The spring-mounting of the model is shown in Fig. 3(b). The driving system of the flaps in the wind tunnel test is different a little from the above-mentioned system in an actual bridge. The model is fixed with the hinge at H_α of the supporting frame and elastically supported by the pitching springs k_α from the frame only allowing a pitching oscillation about the hinge H_α. The frame is supported by the vertical

(a) Cross section of bridge deck system

(b) Spring mount of the bridge deck system

(c) Flap angles due to deformation of the bridge deck

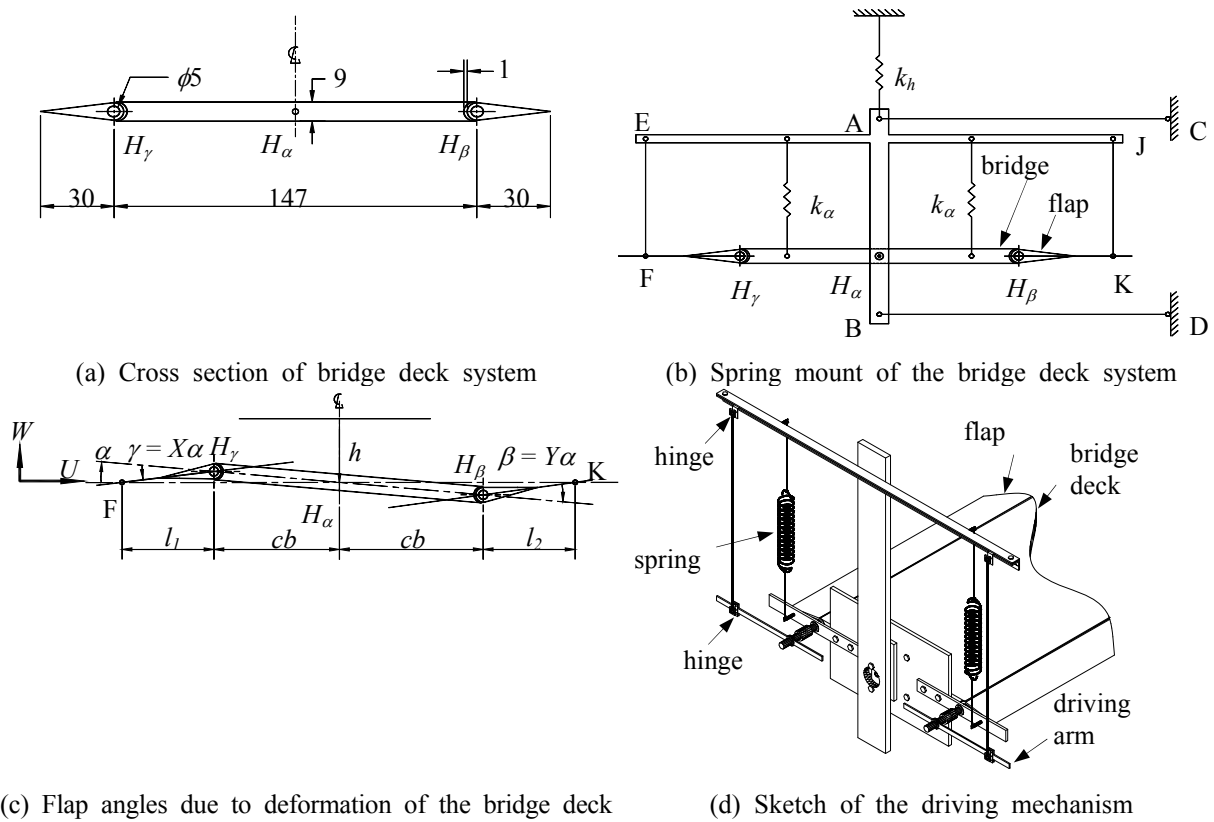(d) Sketch of the driving mechanism

Fig. 3 Wind tunnel model

spring k_h which allows only vertical motion of the frame including the model. The connecting rods AC and BD inhibit the sway motion and rotation of the frame. Thus the model has two degrees of freedom of oscillation, heaving and pitching.

The flap installed at the leading edge of the model has a driving arm FH_γ at its end of the rotation axis of the flap as shown in the figure. The vertical tie bar EF connects between a given point of the driving arm and the frame. The pitching motion of the flap is given by the pitching motion of the bridge deck through the driving arm. The magnitude of the turning angle and turning direction of the leading edge flap depend on the location of the tie bar EF as follows: $X = (cb + l_1)/l_1$; $Y = -(cb + l_2)/l_2$ If $l_1 = l_2$ and $G = (cb + l_1)/l_1$, the controlling angles are $\beta = -G\alpha$, $\gamma = G\alpha$. Thus the control manner as has been described in the above section is realized in this model. During a heaving motion of the model-mounted system, this driving arm does not move. The trailing edge also has the same mechanism. Fig. 3(c) explains the flap displacement when the angle of attack of the bridge deck is given. Fig. 3(d) shows the sketch of the flap driving mechanism.

The model dimensions and dynamic properties are shown in Table 1 in which the weight of the model includes the mass of the frame. The damping ratios are measured when the flaps are fixed.

Vertical wind gust is actively simulated in the Eiffel type wind tunnel based on Karman's spectrum with turbulence intensity of 5% (Kobayashi and Hatanaka 1992, Kobayashi *et al.* 1994). Horizontal wind has no turbulence.

Table 1 Model dimensions and dynamic properties

Parameters		Notation	Value
Length × Width × Depth (mm)		$L \times 2b \times h$	$408 \times 207 \times 9$
Width of flap (mm)		$(1 - c)b$	30
Mass (kg)		m	2.1
Inertia moment (kgm^2)		I	0.0041
Frequency (Hz) (fixed flaps)	Heaving	f_h	0.998
	Pitching	f_α	1.3
Damping ratio (fixed flaps)	Heaving	ξ_h	0.0045
	Pitching	ξ_α	0.028

Table 2 Dynamic properties of system with flaps

Amplification factor		Fixed flaps		Bridge with flap motion							
X	Y	f_h(Hz)	f_α(Hz)	f_h(Hz)	ξ_h	f_α(Hz)	ξ_α	I_γ(kgm^2)	I_β(kgm^2)	I_{total}(kgm^2)
2.29	0	0.998	1.328	0.999	0.004	1.341	0.03	3.45E-05	0	4.02E-03
3	0	0.999	1.331	0.997	0.0036	1.346	0.031	3.03E-05	0	4.01E-03
4	0	1.000	1.329	0.996	0.0035	1.355	0.034	3.89E-05	0	3.94E-03
5	0	0.997	1.33	0.998	0.0041	1.364	0.035	4.04E-05	0	3.89E-03
0	-2.29	0.996	1.33	0.998	0.0045	1.34	0.032	0	2.66E-05	4.05E-03
0	-3	0.997	1.331	0.997	0.004	1.348	0.033	0	3.43E-05	3.99E-03
0	-4	0.998	1.328	0.999	0.0042	1.352	0.035	0	3.61E-05	3.96E-03
0	-5	0.995	1.332	0.998	0.0042	1.361	0.036	0	3.46E-05	3.93E-03

3.3 Experimental flapping forces results

For without control case, $X = Y = 0$, the dynamic properties of method with fixed flaps are measured in still air as shown in Table 2. At a given speed in smooth flow, the model is given an initial displacement, and allowed an oscillation. The accelerations and velocities of heaving and pitching are calculated from measured data. Using the least square method for Eq. (1) in case of without control ($L_{ad} = 0$, $M_{ad} = 0$), H_i and A_i ($i = 1$ to 4) in Eqs. (3) or H_i^*, A_i^* ($i = 1$ to 4) in Eq. (10) can be obtained easily. The results are shown in Fig. 4. Because the test is done in the smooth flow with the coupled motion of heaving and pitching, the sign of A_2^* is changed. At the change point, the flutter happens.

The similarly test is done for the case of with flap motion with the different values of (X, Y). In each case of the test, the parameters of system are measured as shown in Table 2.

The mean inertia moments of leading edge flap and trailing edge flap are about 3.6E-05 kgm^2 and 3.3E-05 kgm^2, respectively. Fig. 5 shows the results of the flap derivatives F_{Li}^*, F_{Mi}^* ($i = 1$ to 4).
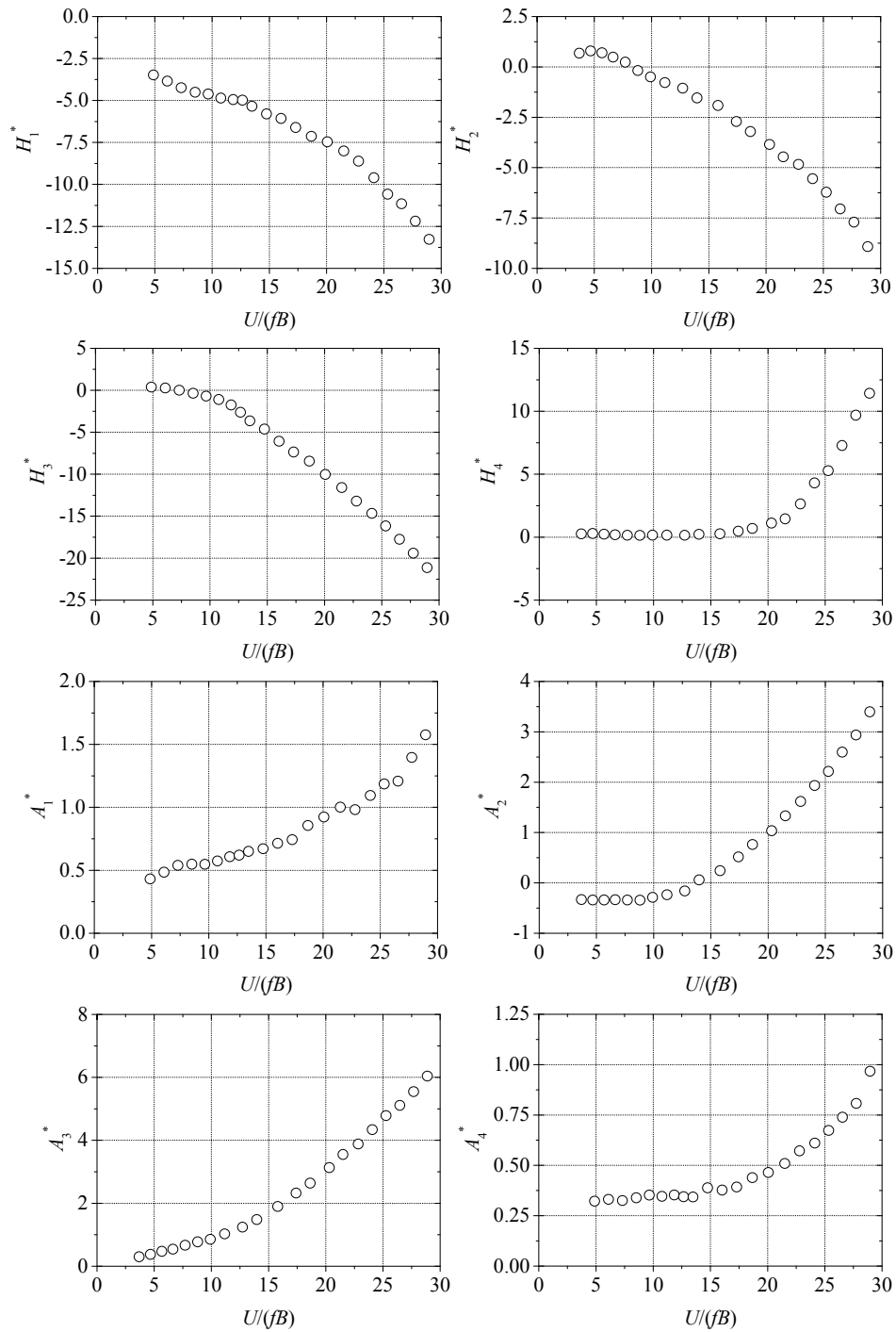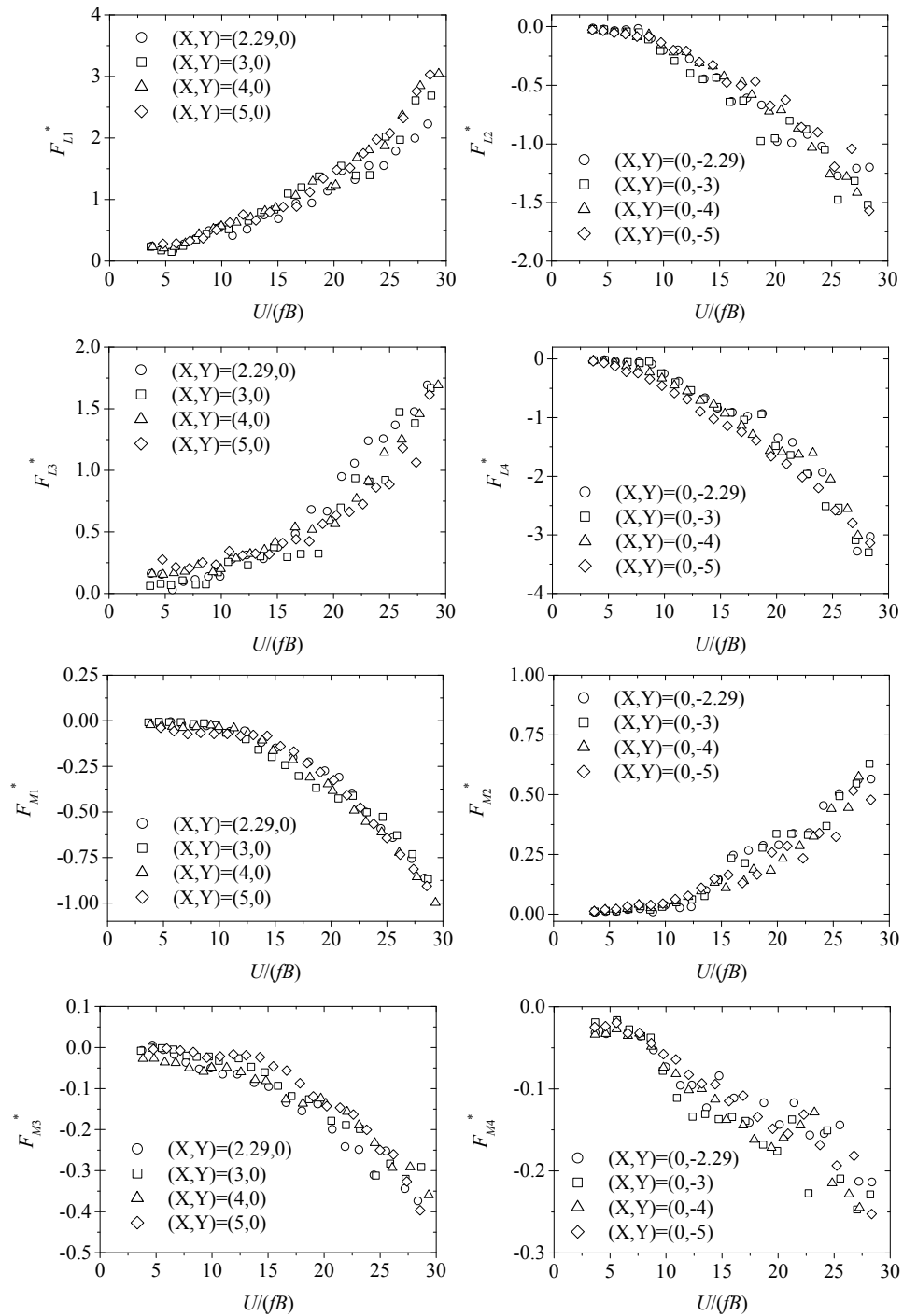
Fig. 4 Flutter derivatives of bridge deck

Fig. 5 Flutter derivatives of flaps

4. Rational function method

The assessment of unsteady aerodynamic forces in the time domain requires identification of aerodynamic impulse or indicial response functions. The techniques for identifying the frequency domain force parameters such as flutter derivatives and admittance functions have been fully established, and a large data set for a host of geometric configurations of bridge sections has been developed (Walshe and Wyatt 1983, Sarkar *et al.* 1994, Bosch 1995, Matsumoto *et al.* 1995, Larose and Mann 1998). However, the flutter derivatives and admittance functions are normally known only at discrete values of reduced frequency *K*. It is difficult to directly use the aforementioned relationships to quantify the impulse or indicial response functions by means of the inverse Fourier transform. Therefore, approximate continuous functions of the reduced frequency are required for describing frequency dependent force parameters for future analysis. For the self-excited forces and the control forces, the rational function approximation technique known as Roger's approximation can be utilized (Wilde *et al.* 1996, Mishra *et al.* 2008, Kirch and Peil 2009, 2011).

4.1 Rational approximation for self-excited forces

Eq. (10) represent the self-excited forces expressed into frequency-time domain for the complex sinusoidal motions with frequency ω in two-dimensional oscillation $h = \bar{h}e^{i\omega t}$, $\alpha = \bar{\alpha}e^{i\omega t}$, and using the Fourier transform ($F[\ldots]$ is the Fourier transform operator) for the lift force of Eq. (10)

$$F\left[L_{se}(t)\right] = \frac{1}{2}\rho U^2 B \left(\frac{KH_1^*}{U}F\left[\dot{h}\right] + \frac{KH_2^*B}{U}F\left[\dot{\alpha}\right] + K^2 H_3^* F\left[\alpha\right] + \frac{K^2 H_4^*}{B}F\left[h\right] \right) \qquad (12)$$

Eq. (12), using $F\left[\dot{h}\right] = i\omega F\left[h\right]$, and similarly for moment, can be written in the compact form as follows

$$\begin{bmatrix} F\left[L_{se}(t)\right] \\ F\left[M_{se}(t)\right] \end{bmatrix} = \frac{1}{2}\rho U^2 \begin{bmatrix} K^2\left(H_4^* + iH_1^*\right) & K^2 B\left(H_3^* + iH_2^*\right) \\ K^2 B\left(A_4^* + iA_1^*\right) & K^2 B^2\left(A_3^* + iA_2^*\right) \end{bmatrix} \begin{bmatrix} F\left[h\right] \\ F\left[\alpha\right] \end{bmatrix} \qquad (13)$$

Starting from the hypotheses that self-excited forces derive from an overlapping of linear mechanisms, some authors propose another straightforward numerical model for self-excited forces in terms of the convolution integral between the structural motion and the impulse response function (Lin and Yang 1983); for the lift force it is

$$L_{se}(t) = \frac{1}{2}\rho U^2 \int_{-\infty}^{t} \left[I_{Lseh}(t-\tau)h(\tau) + I_{Lse\alpha}(t-\tau)\alpha(\tau) \right] d\tau \qquad (14)$$

where I_i indicates the impulse function of the self-exciting forces, which are associated with the indicial aerodynamic functions (Scanlan *et al.* 1974, Scanlan 1984), and the subscripts represent the corresponding force components.

Taking the Fourier transform of Eqs. (14)

$$F\left[L_{se}\left(t\right)\right]=\frac{1}{2}\rho U^{2}\left[F\left[I_{Lseh}\right]F\left[h\right]+F\left[I_{Lse\alpha}\right]F\left[\alpha\right]\right] \tag{15}$$

And similarly for moment, Eq. (13) can be written in the compact form as follows

$$\begin{bmatrix}F\left[L_{se}\left(t\right)\right]\\F\left[M_{se}\left(t\right)\right]\end{bmatrix}=\frac{1}{2}\rho U^{2}\begin{bmatrix}F\left[I_{Lseh}\right]&F\left[I_{Lse\alpha}\right]\\F\left[I_{Mseh}\right]&F\left[I_{Mse\alpha}\right]\end{bmatrix}\begin{bmatrix}F\left[h\right]\\F\left[\alpha\right]\end{bmatrix} \tag{16}$$

Comparing between Eq. (13) and Eq. (16), the relationship between the aerodynamic impulse functions and flutter derivatives can be obtained

$$\begin{aligned}K^{2}\left(H_{4}^{*}+iH_{1}^{*}\right)&=\overline{I}_{Lseh}^{*}=F\left[I_{Lseh}\right]\\K^{2}B\left(H_{3}^{*}+iH_{2}^{*}\right)&=B\overline{I}_{Lse\alpha}^{*}=F\left[I_{Lse\alpha}\right]\\K^{2}B\left(A_{4}^{*}+iA_{1}^{*}\right)&=B\overline{I}_{Mseh}^{*}=F\left[I_{Mseh}\right]\\K^{2}B^{2}\left(A_{3}^{*}+iA_{2}^{*}\right)&=B^{2}\overline{I}_{Lse\alpha}^{*}=F\left[I_{Mse\alpha}\right]\end{aligned} \tag{17}$$

Using Roger's approximation (Roger 1977) for the self-excited forces, for example

$$\overline{I}_{Lseh}^{*}\left(i\omega\right)=a_{0,Lh}+a_{1,Lh}\left(iK\right)+a_{2,Lh}\left(iK\right)^{2}+\sum_{g=3}^{n}a_{g,Lh}\frac{iK}{iK+d_{g,Lh}} \tag{18}$$

where $a_{0,Lh}$, $a_{1,Lh}$, $a_{2,Lh}$, $a_{g,Lh}$, and $d_{g,Lh}$ ($d_{g,Lh}\geq0$, $g=3$ to n) are frequency independent coefficients; the first and second terms represent non-circulatory static-aerodynamics and the aerodynamic damping, respectively; the third term denotes the additional aerodynamic mass that is normally negligible; and the rational terms represent the unsteady components that lag the velocity term and permit an approximation of the time delays through positive values of the parameter $d_{g,Lh}$. The value of n determines the level of accuracy of this approximation and the size of additional equations [given in Eq. (24)]. All of the coefficients in (18) can be determined by the linear and nonlinear least squares methods using the experimentally obtained flutter derivatives at different reduced frequencies.

Replace $s=i\omega$, take inverse Laplace transform of Eq. (18)

$$\begin{aligned}I_{Lseh}\left(t\right)=\Im^{-1}\left[\overline{I}_{Lseh}^{*}\left(s\right)\right]&=a_{0,Lh}\delta\left(t\right)+a_{1,Lh}\frac{B}{U}\dot{\delta}\left(t\right)+a_{2,Lh}\left(\frac{B}{U}\right)^{2}\ddot{\delta}\left(t\right)\\&+\sum_{g=3}^{n}a_{g,Lh}\left[\delta\left(t\right)-\frac{d_{g,Lh}U}{B}e^{\left(-\frac{d_{g,Lh}U}{B}t\right)}\right]\end{aligned} \tag{19}$$

Substituting Eq. (19) into Eq. (14) for $I_{Lseh}(t)$, we can find the self-excited force $L_{seh}(t)$ in time domain.

$$L_{seh}\left(t\right)=\frac{1}{2}\rho U^{2}\left(a_{0,Lh}h\left(t\right)+a_{1,Lh}\frac{B}{U}\dot{h}\left(t\right)+a_{2,Lh}\left(\frac{B}{U}\right)^{2}\ddot{h}\left(t\right)+\sum_{g=3}^{n}\psi_{L,gh}\left(t\right)\right) \tag{20}$$

Similarly, the other self-excited lifts and moments are

$$L_{se\alpha}(t) = \frac{1}{2}\rho U^2 B \left(a_{0,L\alpha} h(t) + a_{1,L\alpha} \frac{B}{U} \dot{h}(t) + a_{2,L\alpha} \left(\frac{B}{U} \right)^2 \ddot{h}(t) + \sum_{g=3}^{n} \psi_{L,g\alpha}(t) \right) \tag{21}$$

$$M_{seh}(t) = \frac{1}{2}\rho U^2 B \left(a_{0,Mh} h(t) + a_{1,Mh} \frac{B}{U} \dot{h}(t) + a_{2,Mh} \left(\frac{B}{U} \right)^2 \ddot{h}(t) + \sum_{g=3}^{n} \psi_{M,gh}(t) \right) \tag{22}$$

$$M_{se\alpha}(t) = \frac{1}{2}\rho U^2 B \left(a_{0,M\alpha} h(t) + a_{1,M\alpha} \frac{B}{U} \dot{h}(t) + a_{2,M\alpha} \left(\frac{B}{U} \right)^2 \ddot{h}(t) + \sum_{g=3}^{n} \psi_{M,g\alpha}(t) \right) \tag{23}$$

where the memory term ψ is new variable that is introduced to express the aerodynamic phase lag and can be found as follows

$$\psi_{x,gy}(t_j) = b_{g,xy}\psi_{x,gy}(t_{j-1}) + a_{g,xy}c_{g,xy}\dot{y}(t_{j-1})\Delta t \tag{24}$$

where x is L or M, and y is h or α, the component $\Delta t = t_j - t_{j-1}$ and

$$b_{g,xy} = \exp\left[-d_{g,xy} \frac{U}{B} \Delta t \right]$$

$$c_{g,xy} = \exp\left[-d_{g,xy} \frac{U}{2B} \Delta t \right] \tag{25}$$

To find the coefficients of aerodynamic forces $a_{j,xy}$ ($j = 0$ to n) and $d_{g,xy}$ ($g = 3$ to n), the nonlinear least squares fit method is used. The general case of $\overline{I}^*_{xsey}$ in Eq. (17) is

$$\overline{I}^*_{xsey} = K^2 \left(\varphi^* + i\phi^* \right) = \lambda_0 + \lambda_1(iK) + \lambda_2(iK)^2 + \sum_{g=3}^{n} \lambda_g \frac{iK}{iK + d_g} \tag{26}$$

For example, choose $n = 6$, separating the real and imaginary parts in Eq. (26) and replace $K = 1/\varepsilon$ yields

$$\varphi^* = \lambda_0\varepsilon^2 - \lambda_2 + \frac{\lambda_3\varepsilon^2}{1 + \varepsilon^2 d_3^2} + \frac{\lambda_4\varepsilon^2}{1 + \varepsilon^2 d_4^2} + \frac{\lambda_5\varepsilon^2}{1 + \varepsilon^2 d_5^2} + \frac{\lambda_6\varepsilon^2}{1 + \varepsilon^2 d_6^2}$$

$$\phi^* = \lambda_1\varepsilon + \frac{\lambda_3 d_3\varepsilon^3}{1 + \varepsilon^2 d_3^2} + \frac{\lambda_4 d_4\varepsilon^3}{1 + \varepsilon^2 d_4^2} + \frac{\lambda_5 d_5\varepsilon^3}{1 + \varepsilon^2 d_5^2} + \frac{\lambda_6 d_6\varepsilon^3}{1 + \varepsilon^2 d_6^2} \tag{27}$$

With known values of ϕ^* and φ^* at discrete point K from wind tunnel testing in smooth flow, Eq. (27) can be solved by the least square method and the coefficients of aerodynamic forces are found.

Summing lifts and moments from Eq. (20) to Eq. (23), the self-excited forces acting on bridge deck in time domain are

Table 3 Approximation coefficients of self-excited forces

i	$a_{i,Lh}$	$a_{i,L\alpha}$	$a_{i\,Mh}$	$a_{i\,M\alpha}$	$d_{i,Lh}$	$d_{i,L\alpha}$	$d_{i\,Mh}$	$d_{i\,M\alpha}$
0	0.466	-1.045	0.048	0.180	-	-	-	-
1	-2.348	-2.302	0.139	0.373	-	-	-	-
2	1.656	-0.712	-0.423	0.666	-	-	-	-
3	-1.322	3.388	0.139	-1.195	20.695	17.075	20.468	15.998
4	-0.897	3.326	0.138	-1.203	20.098	17.033	20.465	15.992
5	-2.464	3.330	0.143	-1.205	20.485	17.092	20.470	15.988
6	4.045	3.269	0.138	-1.204	20.656	17.003	20.461	15.990

$$L_{se} = Q_{se0}\frac{\pi}{B}\left[\frac{a_{2,Lh}}{2\pi}\frac{B}{U^2}\ddot{h} + \frac{a_{2,L\alpha}}{2\pi}\left(\frac{B}{U}\right)^2\ddot{\alpha} + \frac{a_{1,Lh}}{2\pi}\frac{\dot{h}}{U} + \frac{a_{1,L\alpha}}{2\pi}\frac{B\dot{\alpha}}{U} + \frac{a_{0,L\alpha}}{2\pi}\alpha + \frac{a_{0,Lh}}{2\pi}\frac{h}{B} + \Phi_{Lse}\right]$$

$$M_{se} = Q_{se0}\frac{\pi}{4}\left[\frac{2a_{2,Mh}}{\pi}\frac{B}{U^2}\ddot{h} + \frac{2a_{2,M\alpha}}{\pi}\left(\frac{B}{U}\right)^2\ddot{\alpha} + \frac{2a_{1,Mh}}{\pi}\frac{\dot{h}}{U} + \frac{2a_{1,M\alpha}}{\pi}\frac{B\dot{\alpha}}{U} + \frac{2a_{0,M\alpha}}{\pi}\alpha + \frac{2a_{0,Mh}}{\pi}\frac{h}{B} + \Phi_{Mse}\right]$$

(28)

where $Q_{se0} = \rho B^2 U^2$; and

$$\Phi_{Lse} = \frac{1}{2\pi}\left[\frac{1}{B}\sum_{g=3}^{n}\psi_{L,gh} + \sum_{g=3}^{n}\psi_{L,g\alpha}\right]$$

$$\Phi_{Mse} = \frac{2}{\pi}\left[\frac{1}{B}\sum_{g=3}^{n}\psi_{M,gh} + \sum_{g=3}^{n}\psi_{M,g\alpha}\right]$$

(29)

Basing on the flutter derivatives of bridge deck at the discrete point K as shown in Fig. 4, using the nonlinear least squares fit method, the values of approximation coefficients of self-excited forces can be obtained and listed in Table 4 for case of $n = 6$.

4.2 Rational approximation for flap forces

Using the same method presented above, the flapping forces of Eq. (11) can be written as

$$L_{ad} = Q_{se0}\frac{\pi}{B}\left[\begin{array}{l}\dfrac{a_{2,L\beta}}{2\pi}\left(\dfrac{B}{U}\right)^2\ddot{\beta} + \dfrac{a_{2,L\gamma}}{2\pi}\left(\dfrac{B}{U}\right)^2\ddot{\gamma} \\[2mm] + \dfrac{a_{1,L\beta}}{2\pi}\dfrac{B\dot{\beta}}{U} + \dfrac{a_{1,L\gamma}}{2\pi}\dfrac{B\dot{\gamma}}{U} + \dfrac{a_{0,L\beta}}{2\pi}\beta + \dfrac{a_{0,L\gamma}}{2\pi}\gamma + \Phi_{Lad}\end{array}\right]$$

$$M_{ad} = Q_{se0}\frac{\pi}{4}\left[\begin{array}{l}\dfrac{2a_{2,M\beta}}{\pi}\left(\dfrac{B}{U}\right)^2\ddot{\beta} + \dfrac{2a_{2,M\gamma}}{\pi}\left(\dfrac{B}{U}\right)^2\ddot{\gamma} \\[2mm] + \dfrac{2a_{1,M\beta}}{\pi}\dfrac{B\dot{\beta}}{U} + \dfrac{2a_{1,M\gamma}}{\pi}\dfrac{B\dot{\gamma}}{U} + \dfrac{2a_{0,M\beta}}{\pi}\beta + \dfrac{2a_{0,M\gamma}}{\pi}\gamma + \Phi_{Mad}\end{array}\right]$$

(30)

where

Table 4 Approximation coefficients of flapping forces

i	$a_{i,L\beta}$	$a_{i,L\gamma}$	$a_{i,M\beta}$	$a_{i,M\gamma}$	$d_{i,L\beta}$	$d_{i,L\gamma}$	$d_{i,M\beta}$	$d_{i,M\gamma}$
0	-0.156	0.070	-0.010	-0.017	-	-	-	-
1	-0.366	0.604	0.140	-0.214	-	-	-	-
2	-0.051	-0.027	0.038	-0.006	-	-	-	-
3	0.484	-0.530	-0.196	0.337	20.002	19.499	19.711	20.141
4	0.461	-0.531	-0.195	0.335	19.986	19.501	19.716	20.137
5	0.477	-0.539	-0.194	0.336	19.984	19.495	19.717	20.138
6	0.458	-0.532	-0.195	0.336	19.971	19.492	19.714	20.139

$$\Phi_{Lad} = \frac{1}{2\pi}\left[\sum_{g=3}^{n}\psi_{L,g\beta} + \sum_{g=3}^{n}\psi_{L,g\gamma}\right]$$

$$\Phi_{Mad} = \frac{2}{\pi}\left[\sum_{g=3}^{n}\psi_{M,g\beta} + \sum_{g=3}^{n}\psi_{M,g\gamma}\right] \tag{31}$$

From the plots in Fig. 5, the values of approximation coefficients of flapping forces can be obtained and listed in Table 4 for case of $n = 6$.

5. Experiment and numerical simulation

5.1 Control method

In the equation of motion Eq. (1), with the effect of the turbulent flow, the total force and moment are

$$L_T = L_{se} + L_{ad} + L_b$$
$$M_T = M_{se} + M_{ad} + M_b \tag{32}$$

where L_b and M_b are buffeting force and buffeting moment, respectively.

The time domain formulation of aerodynamics forces, self-excited forces and flapping forces, are obtained through the rational function approximation, Eq. (28) and Eq. (30), with the approximation coefficients were found and listed in Table 3 and Table 4. The buffeting forces are treated by using the quasi-static theory. If the flaps are driving by Eq. (5), Eq. (1) become

$$\ddot{h} + 2\xi_h\omega_h\dot{h} + \omega_h^2 h = -\frac{Q_{se0}}{m}\frac{\pi}{B}\left[\overline{H}_1\frac{B\ddot{h}}{U^2} + \overline{H}_2\frac{B^2\ddot{\alpha}}{U^2} + \overline{H}_3\frac{\dot{h}}{U} + \overline{H}_4\frac{B\dot{\alpha}}{U} + \overline{H}_5\alpha + \overline{H}_6\frac{h}{B} + \overline{H}_7 + \Phi_L\right]$$

$$\ddot{\alpha} + 2\xi_\alpha\omega_\alpha\dot{\alpha} + \omega_\alpha^2\alpha = \frac{Q_{se0}}{I}\frac{\pi}{4}\left[\overline{A}_1\frac{B\ddot{h}}{U^2} + \overline{A}_2\frac{B^2\ddot{\alpha}}{U^2} + \overline{A}_3\frac{\dot{h}}{U} + \overline{A}_4\frac{B\dot{\alpha}}{U} + \overline{A}_5\alpha + \overline{A}_6\frac{h}{B} + \overline{A}_7 + \Phi_M\right] \tag{33}$$

where $\overline{H}_i$, $\overline{A}_i$ ($i = 1$ to 7) are given by

$$\bar{H}_1 = \frac{1}{2\pi} a_{2,Lh} \qquad\qquad \bar{A}_1 = \frac{2}{\pi} a_{2,Mh}$$

$$\bar{H}_2 = \frac{1}{2\pi}\left(a_{2,L\alpha} + a_{2,L\gamma}X + a_{2,L\beta}Y\right) \quad \bar{A}_2 = \frac{2}{\pi}\left(a_{2,M\alpha} + a_{2,M\gamma}X + a_{2,M\beta}Y\right)$$

$$\bar{H}_3 = \frac{1}{2\pi} a_{1,Lh} \qquad\qquad \bar{A}_3 = \frac{2}{\pi} a_{1,Mh}$$

$$\bar{H}_4 = \frac{1}{2\pi}\left(a_{1,L\alpha} + a_{1,L\gamma}X + a_{1,L\beta}Y\right) \quad \bar{A}_4 = \frac{2}{\pi}\left(a_{1,M\alpha} + a_{1,M\gamma}X + a_{1,M\beta}Y\right) \qquad (34)$$

$$\bar{H}_5 = \frac{1}{2\pi}\left(a_{0,L\alpha} + a_{0,L\gamma}X + a_{0,L\beta}Y\right) \quad \bar{A}_5 = \frac{2}{\pi}\left(a_{0,M\alpha} + a_{0,M\gamma}X + a_{0,M\beta}Y\right)$$

$$\bar{H}_6 = \frac{1}{2\pi} a_{0,Lh} \qquad\qquad \bar{A}_6 = \frac{2}{\pi} a_{0,Mh}$$

$$\bar{H}_7 = \frac{1}{2\pi}\frac{WC'_{L\alpha}}{U} \qquad\qquad \bar{A}_7 = \frac{2}{\pi}\frac{WC'_{M\alpha}}{U}$$

and the augmented aerodynamic states

$$\Phi_L = \Phi_{Lse} + \Phi_{Lad}$$
$$\Phi_M = \Phi_{Mse} + \Phi_{Mad} \qquad (35)$$

5.2 Solution of control parameters

The sensitivity numerical study about the critical speed was done with the combination of the coefficients $X = G$ and $Y = -G$ where G varies from -10.0 to 10.0. The instability phenomenon, it may be flutter, divergence, or large buffeting response, of the bridge deck is defined when pitching response exceeds 0.17radians in *RMS*. The wind speed at this phenomenon is called the critical speed U_{cr}. The equations of motion are solved by Runge-Kutta method. The horizontal wind speed U does not vary with time. The vertical wind $W = \bar{W} + w(t)$ has zero mean $\bar{W} = 0$. The vertical gust $w(t)$ is derived from the Von-Karman's spectrum with turbulence intensity of 5%.

Fig. 6, in which vertical axis shows the critical speed compared with that of no control case $U_{cr,0}$, shows the variation of the critical wind speed due to the gain of the control surfaces, G. Increase in positive gain results in the improvement of the critical wind speed. The maximum ratio $U_{cr} / U_{cr,0}$ is about 2 when G varies from -10.0 to 10.0. Further negative decrease of the gain G decreases the critical wind speed. For the gain G smaller than 0, the flutter wind speed becomes smaller than the flutter wind speed of the bridge deck without the control system.

To check the effect of G on buffeting, the percentage of reduction effect of buffeting response (*PRE*) are introduced

$$PRE_x = \left(\frac{RMS_{c0} - RMS_{cc}}{RMS_{c0}}\right)_x \times 100\% \qquad (36)$$

where RMS_{cc}, RMS_{c0} = root mean square of buffeting response for with and without control case, respectively; subscript x indicates the heaving h or pitching α.
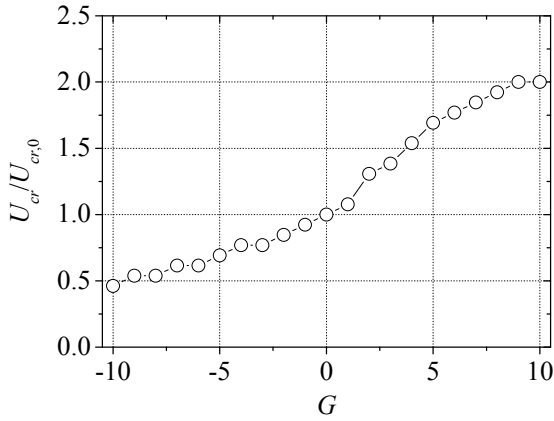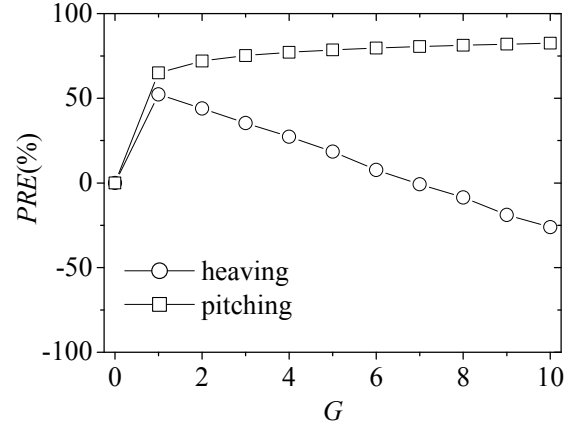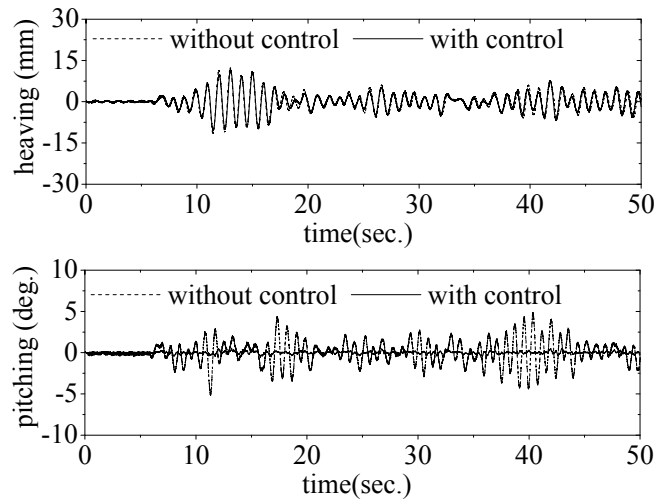
Fig. 6 Effects of the amplifying factor G on flutter   Fig. 7 Effects of the amplifying factor G on buffeting

Fig. 8 Time trace of without control $G = 0$ and with control $G = 5$ at $U/(\omega b) = 2.6$

Fig. 7 shows the effect of G on buffeting at the speed around the critical speed of without control case. When G increases, the high values of PRE_α are gotten. PRE_h reduces and gets negative value when $G > 6$.

5.3 Wind tunnel test

The test aimed at verifying the above theoretical derivations and numerical analysis as well as studying the effects of mechanically driven flaps on the responses of bridge deck.

The flaps are driven through Eqs (5) with $(X, Y) = (G, -G)$, where $G = 5$ Fig. 8 shows the measured time series of the response of the model for without and with control cases at reduced wind speed $U/(\omega b)$ of 2.6, where ω is the natural circular frequency of pitching. After controlling, the heaving and pitching buffeting responses are reduced.
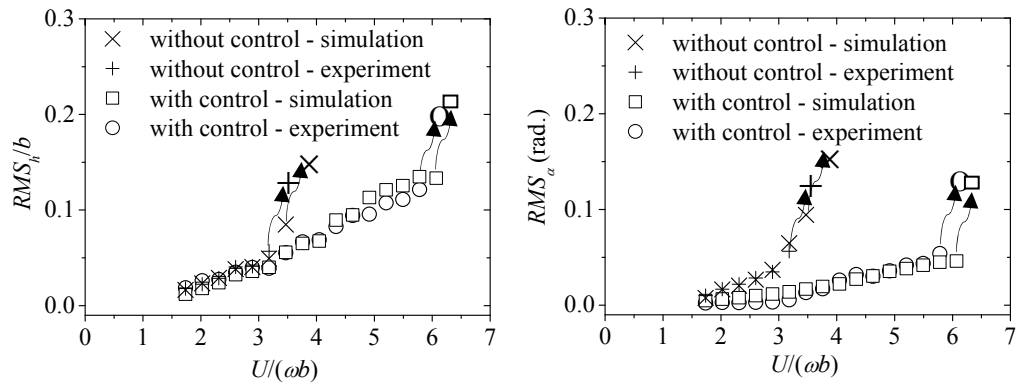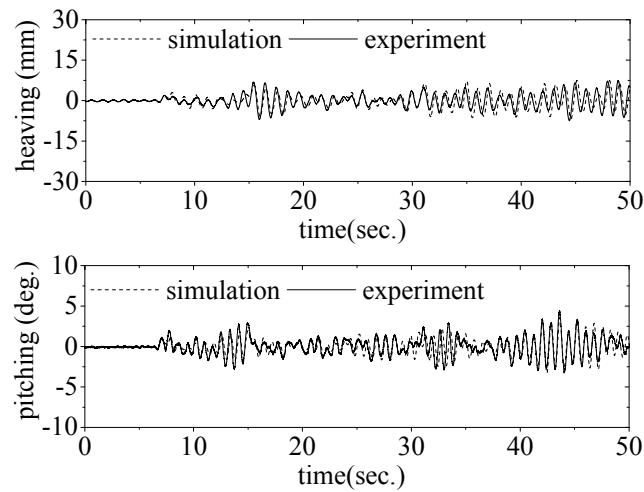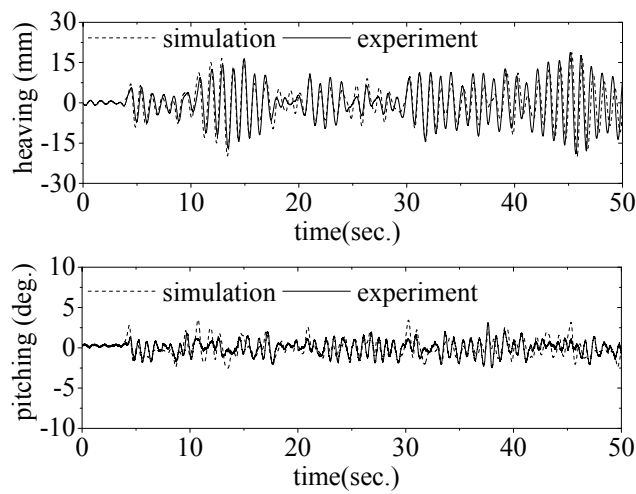
Duc - Huynh Phan and Hiroshi Kobayshi

Fig. 9 *RMS* comparison between numerical and experiment

Fig. 10 Time trace of without control - simulation and experiment at $U/(\omega b) = 2.3$

Fig. 11 Time trace of with control – simulation and experiment $G = 5$ at $U/(\omega b) = 3.76$

The *RMS* amplitude are measured and plotted in Fig. 9, in which the responses obtained in the numerical simulation are included. In the test, the bridge deck without control meets the critical phenomenon at reduced wind speed $U/(\omega b)$ of 3.47. The flaps driven after Eq. (5) could suppress the critical phenomenon up to reduced wind speed $U/(\omega b)$ of 6.07. *RMS* of pitching motion becomes small.

The *RMS* of the response at each wind speed was obtained by numerical calculation. The time series of the model motion at reduced wind speed $U/(\omega b)$ of 2.3 for without control case and of 3.76 for with control case are shown in Fig. 10 and Fig. 11, respectively. The trend of the experimental and numerical cases is nearly the same. The response amplitudes by both methods agree well. The experimental results matched the numerical results.

6. Conclusions

In this paper, a passive aerodynamic control by using mechanically driven flaps has been proposed and analytical and experimental studies of bridge deck section have been conducted. A time domain approach for predicting the coupled flutter and buffeting response of bridge deck with flaps was investigated. With experimental flutter derivatives of bridge deck and flaps, the derivation of time domain model of self-excited forces and control forces of sectional model was represented by using the rational function approximation. Then, the effectiveness of passive flap control was investigated by the numerical simulation and experiment. The following results were found:

(1) In order to suppress the wind induced motion of a bridge, a bridge deck with mechanically driven flaps was proposed. Flaps are turned mechanically its angle in proportion to the pitching angle of the bridge deck.

(2) The flutter derivatives of forces of bridge deck and flapping forces at the discrete point K were found experimentally. The values of approximation coefficients of self-excited forces and flapping forces were obtained by using the nonlinear least squares fit method.

(3) The mechanically control by flaps with $\beta = -G\alpha$, $\gamma = G\alpha$ could be better because it is not only got the effective control but also easy to install. Increase in positive gain G results in the improvement of the critical wind speed. The maximum ratio $U_{cr}/U_{cr,0}$ is about 2 when G varies from -10.0 to 10.0.

(4) In turbulent flow, control by $G = 5$ could improve the flutter speed about 1.8 times and could suppress the critical phenomenon up to its wind speed. Buffeting in pitching motion was effectively suppressed but heaving motion was not.

(5) The results of numerical simulation by using rational function approximation were matched with the experiment ones.

References

Bosch, H.R. (1995), "Aerodynamic performance of the Deer IsleSedgwick Bridge", *Restructuring: America and Beyond, Proc., Structures Congress XIII*, M. Sanayei, ed., **2**, 1558-1562, ASCE, NewYork.
Brown, W.C. (1996), "Development of the deck for the 3300m span Messina", 15th *IABSE Congr. Rep.*, *IABSE, Zurich*, 1019-1030.
Brown, W.C. (1999), "Long span bridge project - a personal view", *Long-Span Bridges and Aerodynamics*,

Springer.

Dung, N., Miyata, T. and Yamada, H. (1996), "Application of robust control to the flutter of long – span bridges", *J. Struct. Eng.*, **42A**, 847-853.

Gua, M., Chang, C.C., Wua, W. and Xiang, H.F. (1998), "Increase of critical flutter wind speed of long-span bridges using tuned mass dampers", *J. Wind Eng. Ind. Aerodyn.*, **73**, 111-123.

Gua, M., Chena, S.R. and Chang, C.C. (2001), "Parametric study on multiple tuned mass dampers for buffeting control of Yangpu Bridge", *J. Wind Eng. Ind. Aerodyn.*, **89**, 987-1000.

Gua, M., Chena, S.R. and Chang, C.C. (2002), "Control of wind-induced vibrations of long-span bridges by semi-active lever-type TMD", *J. Wind Eng. Ind. Aerodyn.*, **90**, 111-126.

Kirch, A. and Peil, U. (2009) "Fundamental restrictions for the closed-loop control of wind-loaded, slender bridges", *Wind and Structures*, **12**(5), 457-474.

Kirch, A. and Peil, U. (2011), "Transfer function approximation of motion-induced aerodynamic forces with rational functions", *Wind and Structures*, 14(2), 133-151.

Kirch, A., Peil, U. and Borri, C. (2009), "Limits for the control of wind-loaded slender bridges with movable flaps; Part I: Aerodynamic modelling, state-space model and open-loop characteristics of the aeroelastic system", *Proceedings of the 5th European and African Conference on Wind Engineering EACWE 5*, Florence, Italy.

Kirch, A., Peil, U. and Borri, C. (2009), "Limits for the control of wind-loaded slender bridges with movable flaps; Part II: Controller design, closed-loop characteristics of the aeroelastic system and gust alleviation", *Proceedings of the 5th European and African Conference on Wind Engineering EACWE 5*, Florence, Italy.

Kobayashi, H. and Nagaoka, H. (1992), "Active control of flutter of a suspension bridge", *J. Wind Eng. Ind. Aerodyn.*, **41-44**, 143-151.

Kobayashi, H. and Hatanaka, A. (1992), "Active generation of wind gust in a two-dimensional wind tunnel", *J. Wind Eng. Ind. Aerodyn.*, **41-44**, 959-970.

Kobayashi, H., Hatanaka, A. and Ueda, T. (1994), "Active simulation of time histories of strong wind gust in a wind tunnel", *J. Wind Eng. Ind. Aerodyn.*, **53**, 315-330.

Kobayashi, H. and Nitta, Y. (1996), "Active flutter control of suspension bridge by control surfaces", *Third International* Conference *on Motion and Vibration Control*, Chiba, 1-6.

Kobayashi, H., Ogawa, R. and Taniguchi, S. (1998), "Active flutter control of a bridge deck by ailerons", *Proc, 2nd World Conf. on Structural Control*, Kyoto.

Kobayashi, H., Mitani, K. and Ogawa, R. (2001), "Active buffeting control by flaps", *The Fifth Asia-Pacific Conference on Wind Engineering*.

Kobayashi, H. and Phan, D.H. (2005), "Bridge deck flutter control by control surfaces", *Proc, 6th Asia-Pacific Conf. on Wind Engineering*, Seoul, Korea.

Körlin, R. and Starossek, U. (2007), "Wind tunnel test of an active mass damper for bridge decks", *J. Wind Eng. Ind. Aerodyn.*, **95,** 267-277.

Kwon, S.D., Jung, S. and Chang, S.P. (2000), "A new passive aerodynamic control method for bridge flutter", *J. Wind Eng. Ind. Aerodyn.*, **86**, 187-202.

Kwon, S.D. and Park, K.S. (2004), "Suppression of bridge flutter using tuned mass dampers based on robust performance design", *J. Wind Eng. Ind. Aerodyn.*, **92**, 919-934.

Larose, G.L. and Mann, J. (1998), "Gust loading on streamlined bridge decks", *J. Fluids Struct.*, **12**, 511-536.

Lin, Y.K. and Yang. J.N. (1983), "Multimode bridge response to wind excitations", *J. Eng. Mech.*, ASCE, **109**(2), 586-603.

Lin, Y.Y., Cheng, C.M. and Lee C.H. (2000), "A tuned mass damper for suppressing the coupled flexural and torsional buffeting response of long-span bridges", *Eng. Struct.*, **22**, 1195-1204.

Matsumoto, M., Mizuno, K., Okubo, K., Ito, Y. and Matsumiya, H. (2007), "Flutter instability and recent development in stabilization of structures", *Journal of Wind Engineering and Industrial Aerodynamics*, **95**(9-11), 888-907.

Matsumoto, M., Nihara, Y., Kobayashi, Y., Shitato, H. and Hamasaki, H. (1995), "Flutter mechanism and its stabilization of bluff bodies", *Proc., 9th Int. Conf. on Wind Engineering*, New Delhi, India, 827-838.

Mishra, S., Kumar, K. and Krishna, P. (2008), "A study of wind effect on damping and frequency of a long span cable-stayed bridge from rational function approximation of self-excited forces", *Wind and Structures*, **11**(1), 71-73.

Miyata, T., Yamada, H., Dung, N. and Kazama, K. (1994), "On active control and structural response control of the coupled flutter problem for long span bridges", *1st World Conf. on Structural Control*, Los Angeles, California, USA.

Nissen, H.D., Sørensen, P.H. and Jannerup, O. (2004), "Active aerodynamic stabilisation of long suspension bridges", *J. Wind Eng. Ind. Aerodyn.*, **92**, 829-847.

Okada, T., Honke, K., Sugii, K., Shimada, S. and Kobayashi, H. (1998), "Suppression of coupled flutter of a bridge deck by tuned pendulum damper", *Proc, 3rd World Conf. on Structural Control,* Kyoto.

Omenzetter, P., Wilde, K. and Fujino, Y. (2000), "Suppression of wind-induced instabilities of a long span bridge by a passive deck-flaps control system. Part I: Formulation", *J. Wind Eng. Ind. Aerodyn.*, **87**(1), 61-79.

Omenzetter, P., Wilde, K. and Fujino, Y. (2000), "Suppression of wind-induced instabilities of a long span bridge by a passive deck-flaps control system. Part II: Numerical simulations", *J. Wind Eng. Ind. Aerodyn.*, **87**(1), 81-91.

Omenzetter, P., Wilde, K. and Fujino, Y. (2002), "Study of passive deck-flaps flutter control system on full bridge model. I: theory", *J. Eng. Mech.*, **128**(3), 264-279.

Omenzetter, P., Wilde, K. and Fujino, Y. (2002), "Study of passive deck-flaps flutter control system on full bridge model. II: results", *J. Eng. Mech.*, **128**(3), 280-286.

Ostenfeld, K.H. and Larsen, A. (1992), "Bridge engineering and aerodynamics", *Aerodynamics of Large Bridges,* Larsen A. (Ed.), Balkema, Rotterdam.

Peidikman, S. and Mook, D.T. (1998), "On the development of a passive-damping system for wind-excited oscillation of long-span bridges", *J. Wind Eng. Ind. Aerodyn.*, **77-78,** 443-456.

Phan, D.H., Kobayashi, H. (2011), "An experimental study of flutter and buffeting control of suspension bridge by mechanically driven flaps", *Wind and Structures*, **14**(2), 152-163.

Roger, K.L. (1977), "Airplane math modeling methods for active control design", AGARD-CP-228.

Sarkar, P.P., Jones, N.P. and Scanlan, R.H. (1994), "Identification of aeroelastic parameters of flexible bridges", *J. Eng. Mech.*, **120**(8), 1718-1742.

Sato, H., Kusuhara, S., Ogi, K. and Matsufuji, H. (2000), "Aerodynamic characteristics of super long-span bridges with slotted box girder", *J. Wind Eng. Ind. Aerodyn.*, **88**(2-3), 297-306.

Sato, H., Hirahara, N., Fumoto, K., Hirano, S. and Kusuhara, S. (2002), "Full aeroelastic model test of a super long-span bridge with slotted box girder", *J. Wind Eng. Ind. Aerodyn.*, **90**(12-15), 2023-2032.

Scanlan, R.H., Béliveau, J.G. and Budlong, K.S. (1974), "Indicial aerodynamic functions for bridge decks", *J. Engrg. Mech.*, ASCE, **100**(4), 657-672.

Scanlan, R.H. (1984), "Role of indicial functions in buffeting analysis of bridges", *J. Struct. Engrg.*, ASCE, **110**(7), 1433-1446.

Scanlan, R.H. (1978), "The action of flexible bridges under wind. 2: Buffeting theory", *J. Sound and Vibration*, **60**(2), 201-211.

Vaurigaud, B., Manevitch, L.I. and Lamarque, C.H. (2011), "Passive control of aeroelastic instability in a long span bridge model prone to coupled flutter using targeted energy transfer", *Journal of Sound and Vibration*, **330**(11), 2580-2595.

Walshe, D.E., and Wyatt, T.A. (1983), "Measurement and application of the aerodynamic admittance function for a box-girder bridge", *J. Wind. Eng. Ind. Aerodyn.*, **14**, 211-222.

Wilde, K., Fujino, Y. and Kawakami, T. (1999), "Analytical and experimental study on passive aerodynamic control of flutter of a bridge deck", *J. Wind Eng. Ind. Aerodyn.*, **80,** 105-119.

Wilde, K. and Fujino, Y. (1998), "Aerodynamic control of bridge deck flutter by active surfaces", *J. Eng. Mech.*, **124**(7), 718-727.

Wilde, K., Fujino, Y. and Masukawa, J. (1996), "Time domain modeling of bridge deck flutter", *J. Struct. Eng./Earthquake Eng.*, JSCE, 13, 93-104.